



**Proceedings of the Sixth International Conference on
Asian and Pacific Coasts (APAC 2011)**

December 14 – 16, 2011, Hong Kong, China

SHIP WAVE CRESTS IN INTERMEDIATE-DEPTH WATER

C. LEE, B.W. LEE

*Department of Civil and Environmental Engineering, Sejong University, 98 Kunja-dong,
Gwangjin-gu, Seoul 143-747, Republic of Korea*

Y.J. KIM

*Maritime & Coastal Department, Saman Corporation, 546-4 Guui-dong, Gwangjin-gu,
Seoul 143-824, Republic of Korea*

K.O. KO

*Department of Research and Development, Hyundai Engineering and Construction
Company, 102-4 Mabuk-dong, Giheung-gu, Yongin-si,
Kyeonggi-do 446-716, Republic of Korea*

In this study, we predicted ship wave crest patterns in intermediate-depth water by extending Kelvin's theory with the recursive relation for the dispersion relation in intermediate-depth water. Using the FLOW-3D we tested for two cases that the relative water depths are $kh = 0.86\pi$ and 0.42π . The numerical results showed that, as the water depth became shallower, both the diverging and transverse wave crests were located further behind the ship and the cusp locus angle became larger as 19.60 and 24.81 degrees, respectively. These were because, in shallower water, the Froude number became higher. In other words, as the ship speed increased compared to the gravity-affected long wave speed, all the wave components were located further behind and outside.

1. Introduction

The waves which propagate outward from the ship have two types of crests, i.e., diverging and transverse ones and Kelvin (1887) found that, in deep water, the two types of crests meet at a farthest point with an angle of 19.47 degree (i.e., cusp locus angle) from the ship trajectory. Physical experiments and numerical experiments proved Kelvin's ship wave crests. Coastal engineers need to predict the ship wave crests in shallower water because ship waves may affect mooring boat or damage seawalls when the ship travels in a narrow channel or with a high speed. Ship waves are generated from a moving source (i.e., ship) and these cannot be predicted by the depth-integrated wave equations such as the

Boussinesq equations and the mild-slope equations. Recently, the code FLOW-3D which uses the RANS (Reynolds Averaged Navier-Stokes) equation has been updated to use the moving boundary condition and thus can predict the ship wave propagation.

In this study, we predicted ship wave crest patterns in intermediate-depth water by extending Kelvin's theory with the recursive relation for the dispersion relation in intermediate-depth water. Using the FLOW-3D we tested for two cases that the relative water depth is $kh = 0.86\pi$ and 0.42π and compared the numerical results with analytically obtained wave crest patterns of the present method and Kelvin's method.

2. Extension of Kelvin's approach in intermediate-depth water

The ship waves can be understood as waves propagating outward from the moving source point. The wave crests may be categorized into diverging and transverse waves. The diverging waves look like waves propagating more right- and left-ward than backwards from the ship and the transverse waves look like waves propagating more backward from the ship.

These waves can be understood as the presently-formed crested waves which have arrived at the points starting from different source points at different times before. Figure 1 shows how each wave component propagates from the source to the crest. All the wave rays perpendicularly meet the crest curves. In the figure, θ means the angle of the wave ray from the ship trajectory. The diverging waves have come from the source point more recently than the transverse waves. For example, the diverging wave with $\theta = 90^\circ$ has just come from the source point at the present time. And, the transverse wave with $\theta = 0^\circ$ has come from the source point at the longest time before. Kelvin (1887) found that, in deep water, the diverging and transverse waves meet at a point (i.e., cusp locus) farthest from the ship trajectory with $\theta = 35.26^\circ$. We may define the cusp locus angle α which is the angle between the cusp locus line and the ship trajectory. Here, the cusp locus line means the line connecting the present ship position and the cusp locus. The Kelvin's cusp locus angle is $\alpha = 19.47^\circ$.

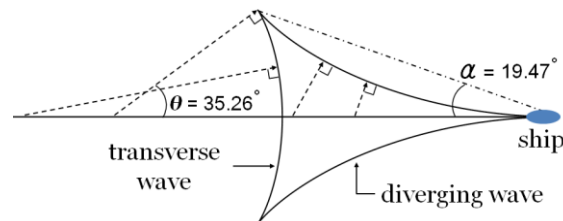


Figure 1. Detailed shape of diverging and transverse waves (Kelvin,1887).

Havelock (1908) found that the cusp locus angle α is different at a different Froude number F_r as follows:

$$\cos^2 \alpha = \begin{cases} \frac{8(1-2kh/\sinh 2kh)}{(3-2kh/\sinh 2kh)^2}, & F_r < 1 \\ 1 - \frac{1}{F_r^2}, & F_r > 1 \end{cases} \quad (1)$$

Here, the Froude number is defined as $F_r = U/\sqrt{gh}$ where U is the ship speed and h is the water depth. The Figure 2 shows the variation of Havelock's cusp locus angles with the Froude number. When the Froude number is less than 0.4, the cusp locus angle is $\alpha = 19.47^\circ$ which was found by Kelvin (1887). As the Froude number increases from $F_r = 0.41$ up to $F_r = 1$, the cusp locus angle increases from $\alpha = 19.48^\circ$ up to $\alpha = 90^\circ$. And, further, as the Froude number increases more than the unity, the cusp locus angle decreases down to $\alpha = 0^\circ$. However, he could not show a detailed crest pattern of diverging and transverse waves as Kelvin did.

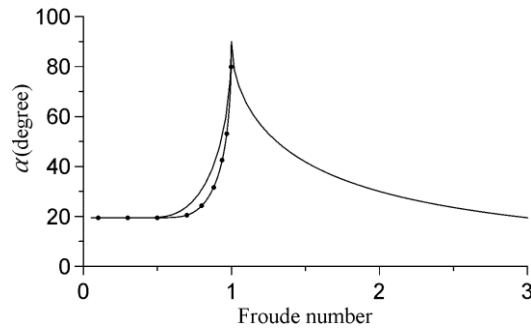


Figure 2. Variation of cusp locus angle with Froude number (Havelock, 1908); solid line = Havelock (1908), solid line with dots = present study.

Here we apply the Kelvin's approach to shallower water and develop a method to show detailed crests of diverging and transverse waves. When a ship travels with a speed U to the $+x$ -direction, the ship wave may be regarded as a group wave travelling from the source point (see Figure 3). Thus, the velocity potential can be defined as

$$\phi = \frac{iga}{\omega} \frac{\cosh k(h+z)}{\cosh kh} e^{i[\omega t - k(X \cos \theta + Y \sin \theta)]} \quad (2)$$

$$X = x + Ut, \quad Y = y, \quad Z = z \quad (3)$$

where (X, Y, Z) and (x, y, z) are the coordinates in a fixed frame and a ship-speed moving frame, respectively, and θ is the angle of the wave ray from the x -axis. In the moving frame, the velocity potential of the ship waves can be defined as

$$\phi = \frac{iga}{\omega} \frac{\cosh k(h+z)}{\cosh kh} e^{i[t(\omega - kU \cos \theta) - k(X \cos \theta + Y \sin \theta)]} \quad (4)$$

The velocity potential will be stationary from the view-point of the ship, thus we get the following relation

$$\omega = kU \cos \theta \quad (5)$$

The linear dispersion of waves is

$$\omega^2 = gk \tanh kh \quad (6)$$

Substituting Eq. (5) into Eq. (6) gives the following equation

$$k = \frac{g}{(U \cos \theta)^2} \tanh kh \quad (7)$$

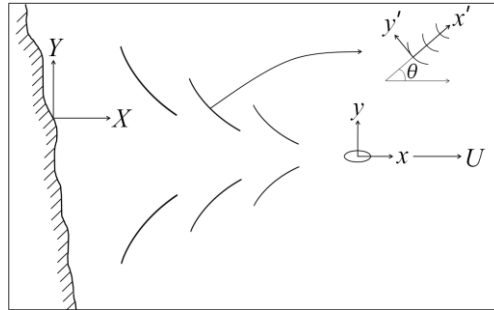


Figure 3. Ship waves in different coordinate systems.

Using the fixed point iteration method, we can obtain the ship wave number in water of intermediate depth. We start with the deep-water wave number k_0 as

$$k_0 = \frac{g}{(U \cos \theta)^2} \quad (8)$$

And, after the i -th iteration, we get

$$k_i = k_0 \tanh k_{i-1} h, \quad i = 1, 2, \dots \quad (9)$$

We use the inclined coordinate (X', Y') normal to the wave crests in a fixed frame. The ship waves will travel in groups such that $d\omega/dk = X'/t$ which can be expressed as

$$\frac{d}{dk}(kX' - \omega t) = 0 \quad (10)$$

where

$$X' = X \cos \theta + Y \sin \theta = x \cos \theta + y \sin \theta + U t \cos \theta \quad (11)$$

Substituting Eq. (11) into Eq. (10), using Eq. (5), and using the chain rule for $k(\theta)$ yield the following equation

$$\frac{d}{d\theta}[k(x \cos \theta + y \sin \theta)] = 0 \quad (12)$$

In deep water, the wave number is $k = k_0 = g/(U \cos \theta)^2$ and thus Eq. (12) can be written as

$$\frac{y}{x} = -\frac{\sin \theta \cos \theta}{1 + \sin^2 \theta} \quad (13)$$

Generally Eq. (13) can be written as

$$\frac{y}{x} = \frac{k \sin \theta - \frac{dk}{d\theta} \cos \theta}{k \cos \theta + \frac{dk}{d\theta} \sin \theta} \quad (14)$$

In water of intermediate depth (i.e., not deep water), wave number depends on the water depth. Substituting Eq. (9) into Eq. (14) gives the following equation

$$\frac{y}{x} = \frac{-(\sin \theta + \sin 3\theta) - \frac{4(\sin \theta + \sin 3\theta)k_0 h}{\sinh(2k_{i-1}h)} \tanh(k_{i-2}h) \left[1 + \dots + \frac{2k_0 h}{\sinh(2k_1 h)} \tanh(k_0 h) \left(1 + \frac{2k_0 h}{\sinh(2k_0 h)} \right) \right]}{5 \cos \theta - \cos 3\theta + \frac{4(\cos \theta - \cos 3\theta)k_0 h}{\sinh(2k_{i-1}h)} \tanh(k_{i-2}h) \left[1 + \dots + \frac{2k_0 h}{\sinh(2k_1 h)} \tanh(k_0 h) \left(1 + \frac{2k_0 h}{\sinh(2k_0 h)} \right) \right]} \quad (15)$$

which can be expressed in x and y as

$$x = \frac{1}{4} C \frac{5 \cos \theta - \cos 3\theta + \frac{4(\cos \theta - \cos 3\theta)k_0 h}{\sinh(2k_{i-1}h)} \tanh(k_{i-2}h) \left[1 + \dots + \frac{2k_0 h}{\sinh(2k_1 h)} \tanh(k_0 h) \left(1 + \frac{2k_0 h}{\sinh(2k_0 h)} \right) \right]}{\tanh(k_{i-1}h)} \quad (16a)$$

$$y = \frac{1}{4} C \frac{-(\sin \theta + \sin 3\theta) - \frac{4(\sin \theta + \sin 3\theta)k_0 h}{\sinh(2k_{i-1}h)} \tanh(k_{i-2}h) \left[1 + \dots + \frac{2k_0 h}{\sinh(2k_1 h)} \tanh(k_0 h) \left(1 + \frac{2k_0 h}{\sinh(2k_0 h)} \right) \right]}{\tanh(k_{i-1}h)} \quad (16b)$$

where C is an arbitrary constant number.

3. Numerical experiments.

Numerical experiments were conducted by the FLOW-3D in order to simulate ship waves in two cases of intermediate-depth waters ($kh = 0.86\pi$ and $kh = 0.42\pi$). Water depth was fixed as $h = 10\text{m}$ and the ship speeds are different as $U = 6\text{ m/s}$ and $U = 8\text{ m/s}$ and the Froude number are $F_r = 0.61$ and $F_r = 0.81$. As the ship speed increases compared to the gravity-affected long wave speed, all the ship wave components would be located further behind and outside and thus the cusp locus angle would increase. Table 1 shows tested ship dimensions which are typical to a yacht in a coastal area.

Table 1. ship dimensions

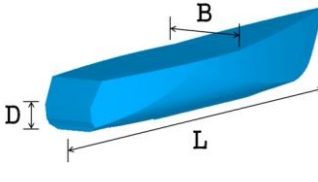
dimension	length (m)	
length overall (L)	8.53	
beam (B)	2.74	
draft (D)	1.00	

Figure 4 shows numerical solutions of the surface elevations by the FLOW-3D for $kh = 0.86\pi$. At this time, the ship was located at $(X, Y) = (560\text{m}, 0\text{m})$. At the initial time the ship started at $(X, Y) = (0\text{m}, 0\text{m})$. This figure shows clearly transverse waves as well as the diverging waves.

Figure 5 compares numerical solutions of the crest points with analytical solutions by the present method (i.e., Eq. (15)) and Kelvin's method (i.e., Eq. (13)). The cusp locus angle was analytically found as $\alpha = 19.60^\circ$ which was not so different from the Kelvin's cusp locus angle of $\alpha = 19.47^\circ$ because the Froude number ($F_r = 0.61$) was much less than the unity.

Figure 6 shows numerical solutions of the surface elevations by the FLOW-3D for $kh = 0.42\pi$. At this time, the ship was located at $(X, Y) = (573\text{m}, 0\text{m})$. This figure shows due to higher speed the ship waves were located further behind the ship and further outside the ship trajectory.

Figure 7 compares numerical solutions of the crest points with analytical solutions by the present method and Kelvin's method. The cusp locus angle was

$\alpha = 24.81^\circ$ which was significantly different from the Kelvin's cusp locus angle of $\alpha = 19.47^\circ$ because the Froude number ($F_r = 0.81$) was close to the unity.

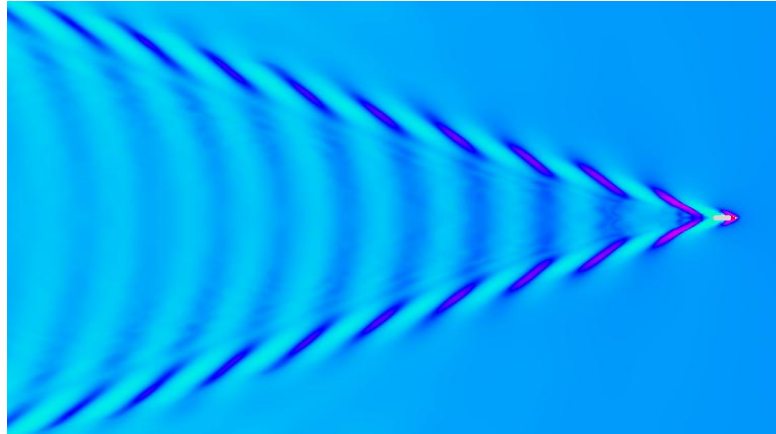


Figure 4. FLOW-3D solution of water surface elevations ($kh = 0.86\pi$, $F_r = 0.61$).

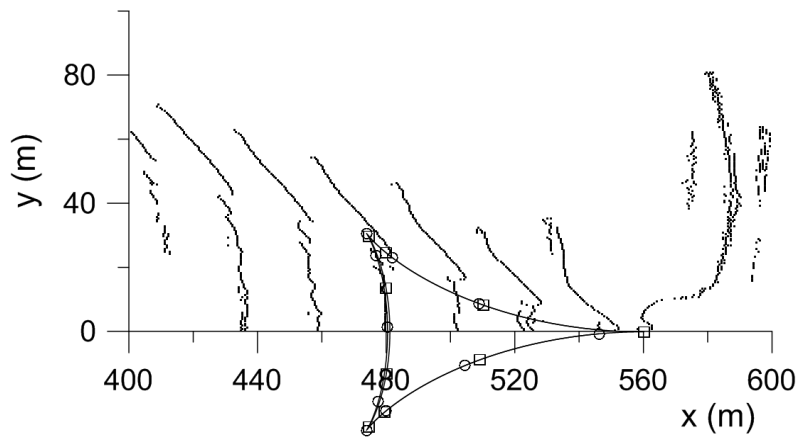


Figure 5. Comparison of FLOW-3D solutions of the crest points with analytical solutions of the present method and Kelvin's method ($kh = 0.86\pi$, $F_r = 0.61$): points = FLOW-3D, \square = Kelvin, \circ = present study.

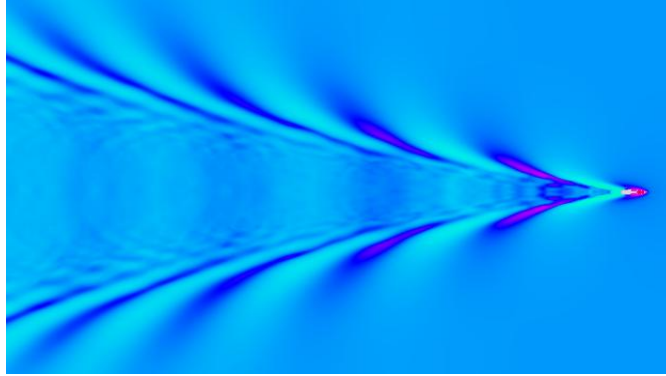


Figure 6. FLOW-3D solution of water surface elevations ($kh=0.42\pi$, $F_r=0.81$).

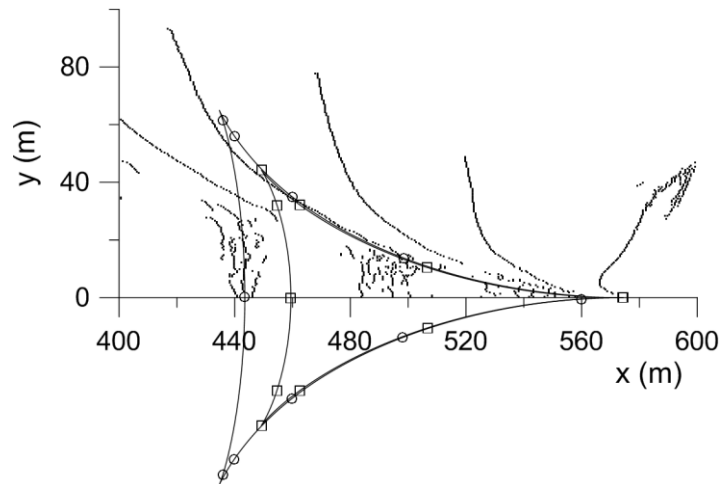


Figure 7. Comparison of FLOW-3D solutions of the crest points with analytical solutions of the present method and Kelvin's method ($kh=0.42\pi$, $F_r=0.81$): points = FLOW-3D, \square = Kelvin, \ominus = present study.

Acknowledgments

This research was supported by the Basic Science Research Program through the National Research Foundation of Korea (NRF) funded by the Ministry of Education, Science and Technology (no.: 2011-0000202).

References

1. T.H. Havelock, *Proc. Royal Soc. London, Series A.*, 398-430 (1908).
2. Lord Kelvin, *Proc. Royal Soc. London*, **42**, 80-83 (1887).